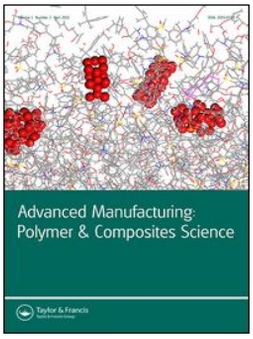

Taylor & Francis
Taylor & Francis Group

Advanced Manufacturing: Polymer & Composites Science

ISSN: (Print) (Online) Journal homepage: https://www.tandfonline.com/loi/yadm20

Efficient cocured scarf repair of composite structures through rheology modeling

David B. Bender & Steven Nutt

To cite this article: David B. Bender & Steven Nutt (2021): Efficient cocured scarf repair of composite structures through rheology modeling, Advanced Manufacturing: Polymer & Composites Science, DOI: 10.1080/20550340.2021.1952046

To link to this article: https://doi.org/10.1080/20550340.2021.1952046

ADVANCED MANUFACTURING: POLYMER & COMPOSITES SCIENCE
https://doi.org/10.1080/20550340.2021.1952046

Taylor & Francis
Taylor & Francis Group

Efficient cocured scarf repair of composite structures through rheology modeling

David B. Bender and Steven Nutt

M.C. Gill Composites Center, Viterbi School of Engineering, University of Southern California, Los Angeles, CA, USA

ABSTRACT

To address the need for increased efficiency and high-quality in-field repair of composite structures, a vacuum bag only (VBO) semi-preg was produced, modeled, and evaluated against a conventional resin and format commonly used for repairs. The semi-preg featured a vinyl hybrid resin formulated for rapid processing with a discontinuous distribution of resin on the fiber bed. The format imparted high through-thickness air permeability relative to conventional out-of-autoclave (OoA) prepregs by virtue of abundant air evacuation pathways with short breathe-out distances. A model was developed to describe the rheological behavior of the resin, and then flow number analysis was employed to assess model accuracy and to guide the design of efficient cure cycles. A custom-built scarfed repair tool featuring an *in situ* observation window was employed to analyze the resin flow and cure process during a scarf repair. Microstructural quality and interlaminar shear strength were compared across the epoxy/vinyl hybrid and conventional/semi-preg panels. The results demonstrated that fast-cure resins can be used in conjunction with flow number analysis and semi-preg formats to design efficient VBO cure cycles that consistently yield patch repairs with low defect contents in repair environments.

KEYWORDS

Prepreg composites; out-of-autoclave prepregs; scarf repair; rheology model

GRAPHICAL ABSTRACT

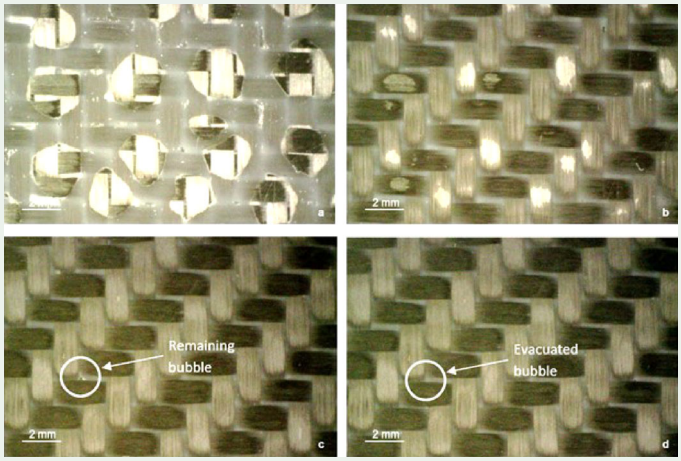

1. Introduction

The objectives of the present work were to modify standard rheology models to accurately predict viscosity behavior of a fast-cure, room-temperature-stable resin, and to assess the impact of resin viscosity on the quality of patch repairs executed with conventional vacuum bag only (VBO) prepregs and semi-pregs (through-thickness air-permeable prepregs). A model was developed to overcome limitations of conventional viscosity profile models and describe the rheological behavior of the fast-cure, room-temperature-stable resin. Flow number analysis was employed to assess the accuracy of the new model and to design tailored cure cycles. Laminates were produced using conventional VBO prepregs and semi-pregs consisting of two resins – an epoxy and a novel resin. Panels then were evaluated for quality and performance. A custom-built tool featuring a transparent window was deployed to provide insight into the resin flow and curing process of a scarfed patch.

Autoclave curing of prepregs has long been the industry standard for producing composite

CONTACT David B. Bender dbender@usc.edu, davebender@sbcglobal.net M.C. Gill Composites Center, Viterbi School of Engineering, University of Southern California, 3651 Watt Way, VHE-402, Los Angeles, CA 90089, USA

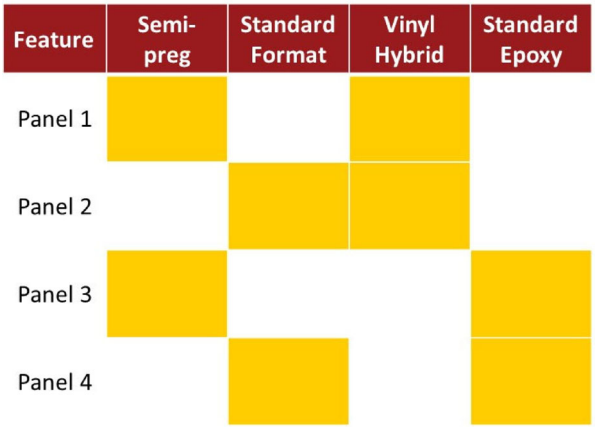

Figure 1. Features of Panels 1–4.

structures for aerospace [1]. The additional pressure applied to laminates inside autoclaves imparts robust quality control [2]. However, the high cost and limited flexibility have encouraged manufacturers to seek out-of-autoclave (OoA) methods of production [3]. Reducing cycle times to eliminate the autoclave bottleneck during production is also sought, provided quality equivalent to autoclave cure can be maintained [4]. Without autoclave pressures, OoA procedures must rely on other methods to suppress/remove volatiles and prevent void formation in laminates [5].

Controlling porosity is key to successful VBO processing of prepregs [6]. Conventional VBO prepregs feature partially impregnated reinforcement with resin on both sides of the fiber bed, creating a vacuum channel in the ply midplane that allows gases to escape through edge-breathing dams [7]. Air and evolved volatiles must be evacuated prior to full saturation and gelation, or voids will remain in the cured laminate [8]. Thus, VBO prepreg plies undergo 'debulking' (extended vacuum holds) to remove gases prior to cure [9]. Debulking does not always remove all gases, and VBO processed laminates often exhibit porosity levels >1%. The need for debulking can extend processing times beyond that of autoclave cure, where the pressure applied reduces the need for extended debulking. Problems with quality control are especially severe when attempting to perform in-field repairs on composites structures [10].

The repair of composite structures presents a unique set of challenges, one of which is the absence of egress pathways at patch edges [11]. The primary limitation of conventional VBO prepregs stems from the complete reliance on edge breathing, and the occlusion of those pathways. Air that has no egress pathway will remain in the laminate as voids, compromising patch strength [12]. Measures such as breathable adhesives and resin infusion have been introduced to promote edge breathing in repair environments, and these approaches have met with varying levels of success [13,14]. Other methods, such as double vacuum debulking (DVD), have also been implemented to reduce porosity in repair patches, albeit at the cost of increased process complexity [15,16]. Volatile management becomes especially difficult when working with in-field conditions. A lack of freezer storage precludes the use of many conventional epoxy prepregs, resulting in deployment of wet layup, a skill-intensive process fraught with human-induced variability [17].

Most repairs employ resins commonly used in the parent structure. Epoxies are the most common thermoset resin used in the aerospace industry, and their rheological behavior is well-characterized [18,19]. However, as epoxy formulations increase in complexity, accurately modeling their rheological behavior has required additional terms in the equations. For instance, Macosko described thermoset viscosity starting with Arrhenius terms [20,21]. However, as epoxy formulations became more diverse, model variations describing viscosity behavior followed. Empirical, molecular, and gel-based models have been developed to describe specific systems [22]. For many modern epoxies, a modified gel model proposed by Khoun has been employed [23]. However, with the advent of thermosets with fast-cure profiles, new models are needed to describe their unique behavior.

In this study, a fast-cure resin and a typical epoxy resin were used to produce (a) conventional prepreg and (b) prepreg with high through-thickness air permeability (semi-preg). Additional terms were introduced to a conventional rheology model to describe the unusual viscosity behavior of the resin. The model was employed in flow number analysis to design efficient cure cycles for the prepregs that were processed with a single vacuum bag in a repair environment, demonstrating how cure cycle parameters (intermediate hold time, intermediate temperature) can be specified to control the quality and performance of cured laminates.

2. Experiments

Two matrix materials were selected, including a vinyl hybrid resin and a conventional prepreg epoxy. Using these resins, four types of panels were produced and analyzed (Figure 1). Panels 1 and 2 were produced using the prototype vinyl hybrid resin. Panel 1 featured semi-preg formatting, while Panel 2 featured conventional OoA prepreg formatting. Two more panels (Panels 3 and 4) were produced using the epoxy resin. Panel 3 featured semi-preg formatting, while Panel 4 featured conventional OoA prepreg formatting. Thus, the four panels consisted of Panel 1 (semi-preg vinyl hybrid), Panel 2

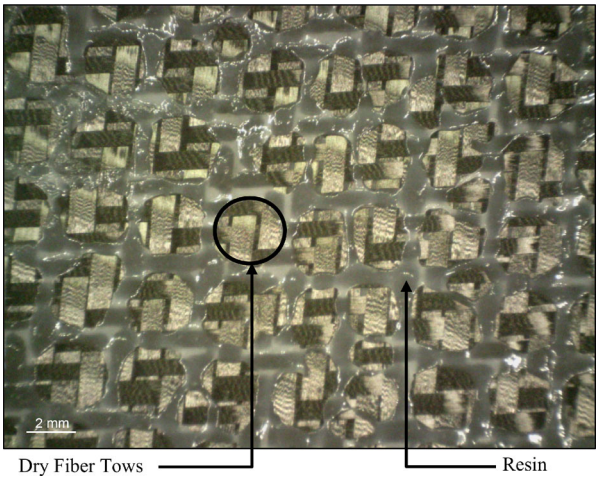

Figure 2. Semi-preg format achieved by applying dewetted film to dry fabric.

(conventional vinyl hybrid), Panel 3 (semi-preg epoxy), and Panel 4 (conventional epoxy).

All panels were cured using VBO processing on a scarf repair tool that allowed for *in situ* observation during cure. Videos of the panels were recorded to document both gas removal and resin flow. Mechanical performance of the panels was evaluated through measurements of interlaminar shear strength (ILSS) because ILSS is a matrix-dominated property. Panel quality was assessed by porosity measurements from five polished sections evenly distributed from each panel.

Panels with vinyl hybrid were fabricated using resin films produced commercially (Tipton-Goss Advanced Materials Company) [24], while panels with epoxy resin were also fabricated using resin films produced commercially (PMT-F4, Patz Materials & Technology). To produce semi-preg formatting, the conventional films were dewetted after nucleation sites were introduced with a hand-held spike roller [25]. The dewetting was conducted on silicone paper in a convection oven (Blue M Oven). The resin was heated in the oven for 2 min at 104 °C until dewetting occurred and established the semi-preg format [26]. Prepreg was then fabricated by transferring either the formatted resin or continuous films to dry fabric (Figure 2).

A tool plate featuring an observation window was deployed to allow *in situ* observation during the cure cycle (Figure 3).

The distinguishing elements of the tool were the 3° scarf incline and the square central observation window. The tool was elevated on legs to accommodate video recording and illumination. Images were recorded at 1 Hz during the early stages of cure, and every 10 s thereafter until resin flow and gas evacuation terminated.

All prepregs were prepared using a 2 × 2 twill fabric of carbon fibers with 6k tows (DowAksa A-

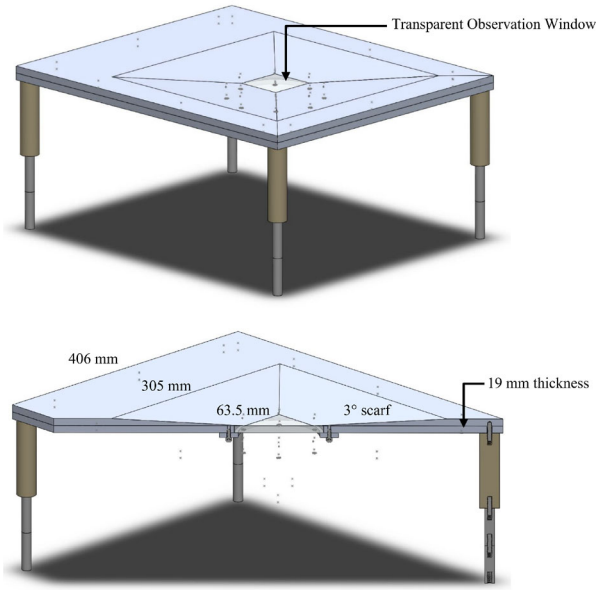

Figure 3. Schematic of repair tool plate with an *in situ* observation window.

38) with resin contents of 35% by weight. A stacking sequence of $[0°/45°]_{2s}$ for 8 plies was used for all panels. The size of the observation window (50 × 50 mm) was the initial ply size. Successive plies were cut proportionally larger to account for the 3° scarf incline to replicate best practices for repairs [27,28]. A transparent release agent (Frekote® 700-NC) was applied to the tool surface before stacking the plies. Perforated release film (Airtech A4000 P8) and a Teflon-coated fiberglass peel ply were placed on top of the laminate, and a nylon breather cloth (Airtech Airweave N10) covered the laminate. Vacuum bagging was then overlaid on the surface and peripherally sealed with sealant tape (Airtech GS213-3). A heat blanket (Briskheat SR512018X18C) was used to heat the laminates after applying vacuum to the bag. A custom control system for temperature control was built using a controller (Watlow PM6R1CA-AAAAAAA), solid state relay (SSR-240-10A-DC1), and K-type thermocouple input. The temperature control of the system was implemented using calibrations of test runs on the blanket system. For the vinyl hybrid panels, the cycle began with a room temperature debulk for 30 min, followed by a 5 °C/min ramp to 93 °C and a 30-min dwell. A second ramp at 5 °C/min to 121 °C was applied and held for 30 min. Cured laminates were cooled to 20 °C at 1.1 °C/min. The same cure cycle was used for the epoxy panels, except that the final hold at 121 °C was 2 h to ensure full cure (unlike the vinyl hybrid, the epoxy was not fast-cure).

Viscosity profiles of the neat resins were measured using a parallel plate rheometer (TA Instruments). Test conditions included five dynamic ramps (1–10 °C/min) up to 150 °C. Results from the

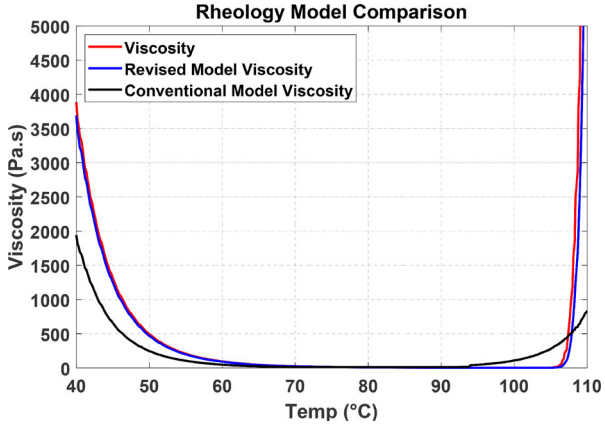

Figure 4. Viscosity profiles of a ramp at 1 °C/min.

rheometer were incorporated into the modeling analysis. Panel quality was assessed by examination of polished sections (25 × 13 mm) from the four panels. Void content was estimated by measuring the ratio of void area to total area in each sample. Panel properties were assessed by measuring ILSS (short-beam-shear, ASTM D2344) using a load frame (Instron 5585H).

3. Results

3.1. Modeling

To describe the rheological properties of vinyl hybrid, equations previously developed to accurately model the cure rate of fast-cure room-temperature-stable resins were used [29]

$$\frac{d\alpha}{dt} = A * \exp\left(\frac{-E_a}{RT}\right) \frac{\alpha^m(\alpha_{max}-\alpha)^n}{1+\exp\left(C(\alpha-(\alpha_{CO}+\alpha_{CT}T))\right)+d(1-\alpha)^h} \quad (1)$$

$$\alpha_{max} = 1 - \frac{1}{1+k*\exp(q*(T_{max}-T_c))} \quad (2)$$

The degree of cure acquired from Equations (1) and (2) was used in the conventional thermoset model for viscosity as a function of temperature (and time) [30]

$$\mu = \mu_1(T) + \mu_2(T)\left(\frac{\alpha_{gel}}{\alpha_{gel}-\alpha}\right)^{(A'+B'\alpha+C'\alpha^2)} \quad (3)$$

$$\mu_i(T) = A_{\mu i}\exp\left(\frac{E_{\mu i}}{RT}\right) \quad i=\{1,2\} \quad (4)$$

Using Equations (3) and (4), multivariable minimization of error was applied to determine values for the constant terms. Systematic discrepancies appeared between the measured viscosity data and values predicted from the model, particularly in early and late stages of cure (Figure 4).

Despite efforts to determine terms that yielded a closer match, differences between measured data and model predictions persisted. The unusual characteristics of the vinyl hybrid resin – room temperature stability and fast cure – were not accounted for adequately in the conventional model, preventing accurate prediction of viscosity behavior, particularly at early and late stages of heating. Viscosity predictions using the conventional model showed a gradual increase beginning at 90 °C, yet measurements showed that the vinyl hybrid did not begin solidifying until 105 °C. Furthermore, the rate at which vinyl hybrid reached its lowest viscosity and its gelation rate were not reflected, leading to a lag on both ends of the viscosity profile.

To resolve these discrepancies and account for both the fast-cure transition (at 105 °C) and the inhibited cure *prior* to transition, slight modifications to the model were required. A term T_c was introduced that reflects the transition temperature of 105 °C, as shown below

$$\mu = \mu_1(T) + \mu_2(T)\left(\frac{\alpha_{gel}}{\alpha_{gel}-\alpha}\right)\left(ye^{z(Tc-T)}\right)(A'+B'\alpha+C'\alpha^2) \quad (5)$$

$$\mu_i(T) = A_{\mu i}\exp\left(\frac{E_{\mu i}}{RT}\right) \quad i=\{1,2\} \quad (6)$$

The transition temperature T_c determined from rheometer measurements was compared with a separate calculation of T_c (a multivariable minimization of error, where T_c was treated as an unknown variable). The value determined from that calculation (105.3 °C) was nearly identical to the value measured using the rheometer. Using the constant values determined from error minimization ($A_{\mu 1} = 8.72e-18$ Pa s, $A_{\mu 2} = 4.23e-3$ Pa s, $E_{\mu 1} = 84672$ J/mol, $E_{\mu 2} = 9462$ J/mol, $A' = 0.46$, $B' = 0.87$, $C' = 3.8$, $\alpha_{gel} = 1$, $y = 2.3$, and $z = -1.32$), yields a phenomenological model that more accurately simulates the viscosity profile of fast-cure resins. Activation energies were reduced, more accurately reflecting the viscosity behavior during initial heating.

The predictions from the modified model Equations (5) and (6) were plotted alongside the measured viscosity, yielding data sets that were closely aligned, with deviation of <5% (Figure 4). In contrast, predictions using the conventional model exhibited deviations >25%.

Using the modified model for viscosity evolution, comparative analysis using flow number was performed. Assuming Newtonian flow prior to gelation, the flow number N_{Fl} can be defined as:

$$N_{Fl} = \left(\frac{\rho_p}{\rho_o}\right)\left[1-\left(\left[\frac{16Fh_o^2}{3\pi R^4}N_{Fl.eff}\right]+1\right)^{-0.5}\right] \times 100 \quad (7)$$

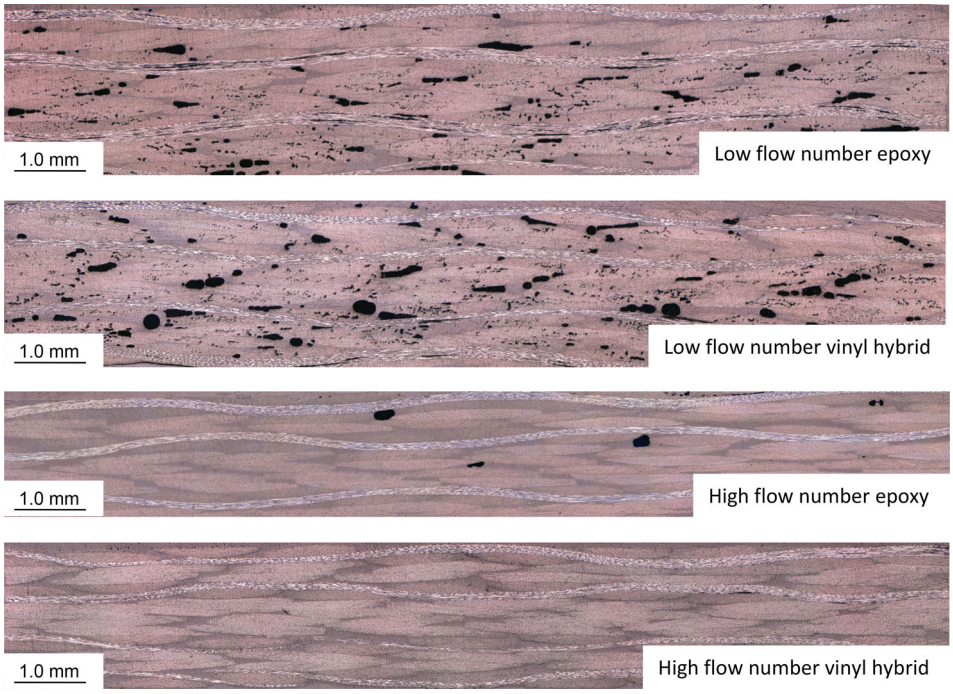

Figure 5. Porosity of fabricated panels with high and low flow numbers.

where ρ_p is the resin density, ρ_p is the prepreg density, F is the lamination force, h_0 is the initial thickness, and R is the effective radius of the resin. The critical part of that expression, the effective flow number $N_{Fl.eff}$ is simply:

$$N_{Fl.eff} = \int_0^{t_{gel}} \eta(t)^{-1} dt \tag{8}$$

where t and η depend on the cure cycle, and a higher $N_{Fl.eff}$ corresponds to increased resin flow [31].

The effective flow number was used to guide the design of cure cycles in this study. For conventional epoxies, the effective flow number encompasses the balance between the decrease in viscosity as temperature increases and the increase in viscosity that accompanies onset of gelation at higher temperatures. These counteracting phenomena severely limit the range of possible effective flow numbers for epoxies. However, vinyl hybrid resin exhibits cure inhibition at temperatures below 105 °C, suppressing the onset of gelation below that temperature. Thus, the resin affords flexibility in design of cure cycles, allowing a wider range of effective flow number.

To evaluate the utility of employing effective flow number to tailor cure cycles, panels were fabricated with the vinyl hybrid and epoxy resins, and cure cycles were specified such that the same effective flow number was achieved for equivalent epoxy and vinyl hybrid panels. Ramp rates, hold times, and temperatures were adjusted to yield the same effective flow number for all panels. Polished sections from four panels were analyzed to measure porosity levels (Figure 5). The first two panels shown correspond to a low flow number regime, one for each material. The remaining two were from a high flow number regime, one for each resin.

The panels show that different materials with the same effective flow number achieved comparable levels of resin infiltration during the cure cycle. For the same low effective flow numbers, similar amount of microporosity was observed in the epoxy and vinyl hybrid panels (~3%). Microporosity in these panels indicated that the resin did not fully saturate the fiber tows, reflecting the low effective flow number. In addition, macro-porosity appeared in the high effective flow number panels because of the limited pathways for air egress. Cure cycles with low effective flow number provided less time for air evacuation prior to gelation. Conversely, panels with high effective flow number exhibited minimal porosity for both the epoxy and vinyl hybrid resins. The primary difference observed between the vinyl hybrid and epoxy panels was the presence of macro-porosity in the epoxy panel stemming from insufficient bubble migration. This issue was explored using *in situ* observation.

Using the modified rheological model for the vinyl hybrid resin, and the conventional rheology model for the epoxy, a cure cycle map was constructed to guide the design of cure cycles. Code was written (MATLAB) to generate normalized flow numbers for simulated cure cycles with a range of parameters. First, the final degree of cure, α_{max}, was determined from Equation (2) and input into the kinetic equation (1) to generate degree of cure, α, at any point in a given cure cycle. Next, the α term and cure cycle parameters were used to generate a normalized flow number using the rheology and

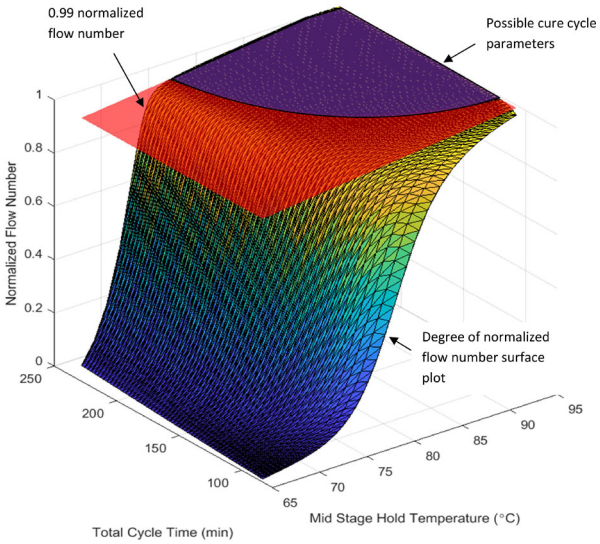

Figure 6. MATLAB plot of cure cycles.

flow number equations (5)–(8). The flow number was normalized to a value of flow number that consistently yielded full saturation from the high flow number panels. Parameters of the cure cycle were varied, including temperature ramp rate, mid-stage hold time, and mid-stage temperature, and the dependence of normalized flow number on intermediate dwell temperature and total cycle time were used to create a 3D plot (Figure 6). In the plot, the red plane represents a flow number of 0.99 and the purple plane indicates possible cure cycles that meet or exceed that value. The normalized flow number values above 1 were displayed as 1 in the figure for clarity.

Through iterations of this process, cure cycles were chosen for the panels that demonstrated the effectiveness of employing semi-preg formatting and increasing effective flow number for reducing/eliminating porosity.

3.2. Repair tool

Samples were cured on the repair tool with the *in situ* observation window to allow observation of resin flow and air evacuation. The images below were selected from video frames recorded during cure of Panel 1, the vinyl hybrid semi-preg laminate (Figure 7).

Figure 7(a) shows the initial resin formatting of the semi-preg, comprised of a resin grid with openings (dry gaps) for through-thickness gas egress. As vacuum was applied and heating/compaction commenced, the resin spread across the fabric, shrinking the openings in the resin (Figure 7(b)). While the air evacuated quickly, a few bubbles remained in the resin prior to gelation (circle in Figure 7(c)). Despite full saturation, the circled bubble continued to shrink in the corner of the fiber tows before eventually disappearing (Figure 7(d)). The low resin viscosity facilitated bubble migration along fiber tows and through the thickness of the laminate. The reduction and eventual elimination of gas bubbles during cure of Panel 1 demonstrated the efficacy of semi-preg formatting, particularly when edge-breathing is restricted or prevented. This feature is particularly relevant to repair environments, especially when combined with a resin that can achieve a high flow number during cure.

The images below were selected from video frames recorded during cure of Panel 3, the epoxy semi-preg laminate (Figure 8).

Figure 8(a) shows resin formatting similar to the vinyl hybrid semi-preg of Figure 7(a). The semi-preg format initially allowed air to escape, reducing the number of bubbles on the laminate surface. When the resin reached full saturation, more bubbles remained compared to the vinyl hybrid panel, and one such bubble is circled in Figure 8(c). However, unlike the bubble in the vinyl hybrid panel, this bubble was unable to escape, resulting in a surface pore (Figure 8(d)). Bubbles were also trapped in the thickness of the laminate.

The images below were selected from video frames recorded during cure of Panel 2, the vinyl hybrid laminate produced with conventional OoA prepreg (Figure 9).

Figure 9(a) shows the initial distribution of resin fully covering the surface of the fabric. As curing began, elongated bubbles or channels formed in between tows (Figure 9(b), arrow). The conventional format of the prepreg alone was not sufficient to prevent bubble formation. The low-viscosity vinyl hybrid resin facilitated bubble escape into the vacuum channels of the plies, and most of these escaped to the laminate edges (Figure 9(c)). However, bubbles often remained on the surface as defects (Figure 9(d), arrow). Prepreg with conventional epoxy displayed the same resin/bubble progression throughout the cure cycle, albeit with more bubbles at the end remaining as defects due to higher resin viscosity.

The micrographs show distinct differences in void characteristics between the four panels (Figure 10).

Panel 1 exhibited negligible porosity, stemming from the semi-preg formatting and the low viscosity of the resin. In contrast, Panel 2 exhibited markedly higher levels of porosity (2.2%), a result attributed to the conventional OoA prepreg format and reliance solely on edge-breathing. The bubbles shown in Figure 9(b–d) were not removed during cure, leading to macro-porosity in the cured laminate (Figure 10(b)). Panel 3 (semi-preg formatting and epoxy resin) exhibited reduced levels of defects

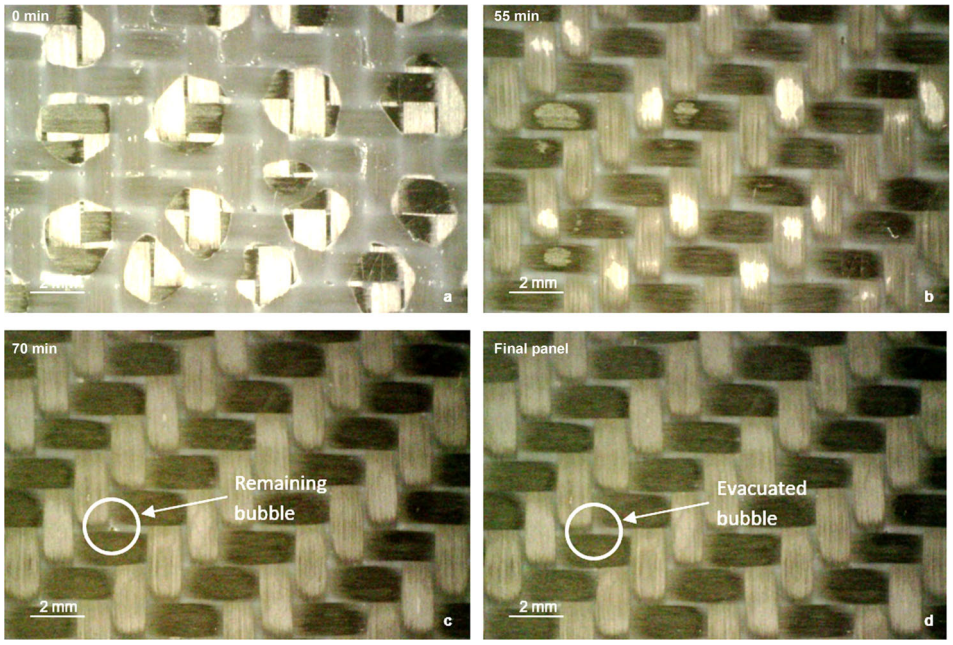

Figure 7. Images acquired in-situ during processing (Panel 1, vinyl hybrid resin).

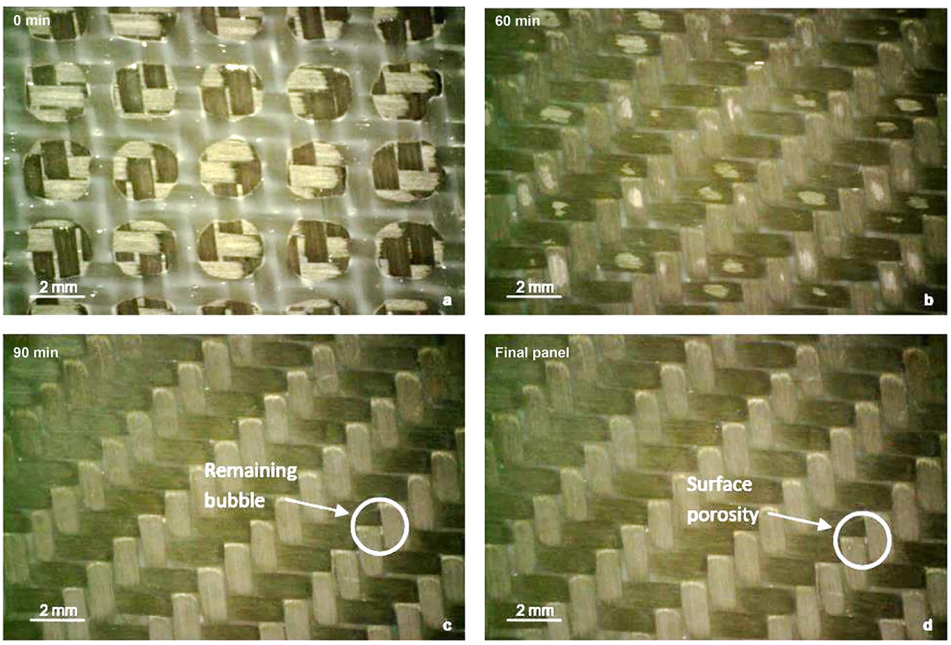

Figure 8. Images acquired *in situ* during processing (Panel 3, epoxy resin).

relative to Panel 2, indicating that while lower-viscosity resins generally facilitate reduction in defect levels, semi-preg formatting is more effective in eliminating porosity. The number and location of macropores in Panel 3 matched the bubbles in the video frames shown previously in Figure 8. Finally, Panel 4 (epoxy resin and conventional OoA prepreg formatting) exhibited higher levels of both micro- and macro-porosity (3.2% and 5.2%).

The graph in Figure 11(a) portrays porosity trends from the polished sections.

Panel 1 (vinyl hybrid semi-preg) exhibited only 0.1% porosity, and most samples showed no voids. In contrast, Panel 2 exhibited 2.2% porosity. The difference between the two panels – primarily the resin formatting of the prepreg plies – was responsible for the higher levels of macro-porosity in Panel 2. Panel 3 exhibited less porosity than Panel 2 (1.2%), despite the fact that the prepreg featured a higher viscosity resin (epoxy) and a cure cycle with a lower flow number. The finding was attributed to the semi-preg formatting of Panel 3, which allowed most gas to escape prior to saturation, much like Panel 1, leading to a reduction in void content. Finally, Panel 4 exhibited 8.4% porosity and the widest range of values between samples. The combination of repair conditions, conventional formatting, and higher viscosity of the epoxy resin in Panel 4, caused the higher levels of porosity.

ILSS is an important measure of mechanical performance and is a matrix-dominated property.

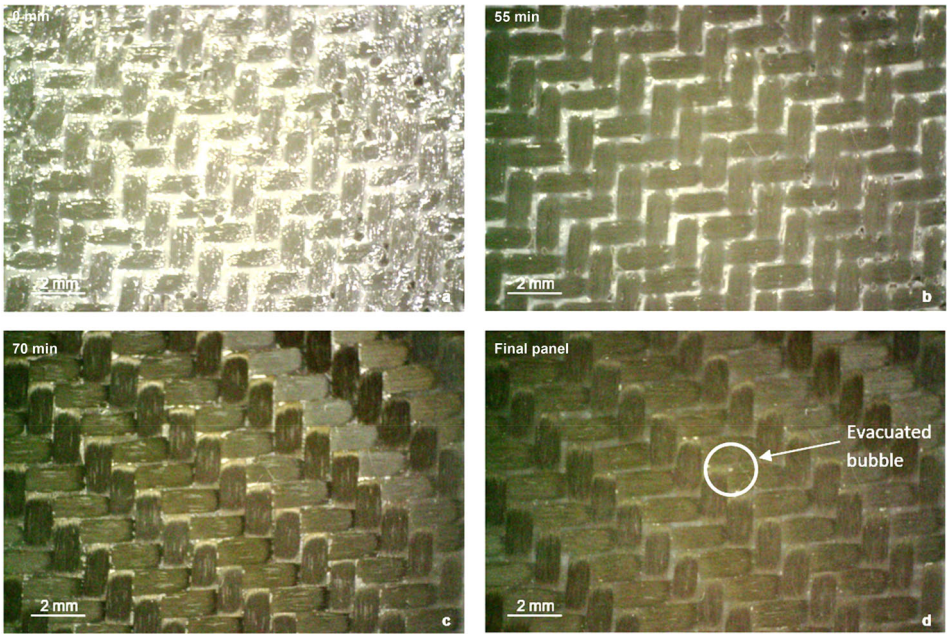

Figure 9. Images acquired *in situ* during processing (Panel 2, vinyl hybrid resin).

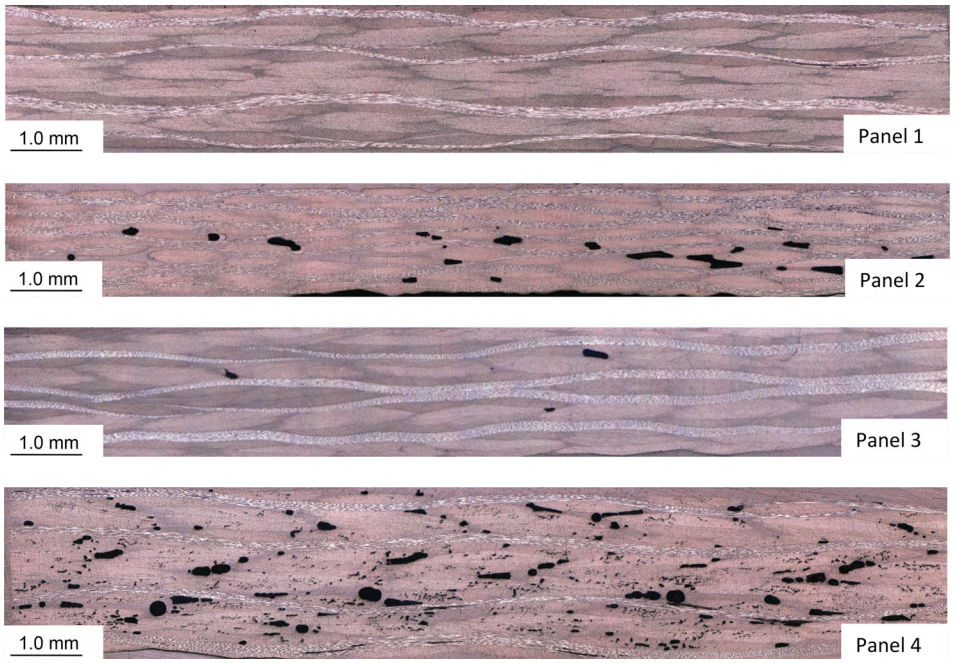

Figure 10. Micrographs of fabricated panels.

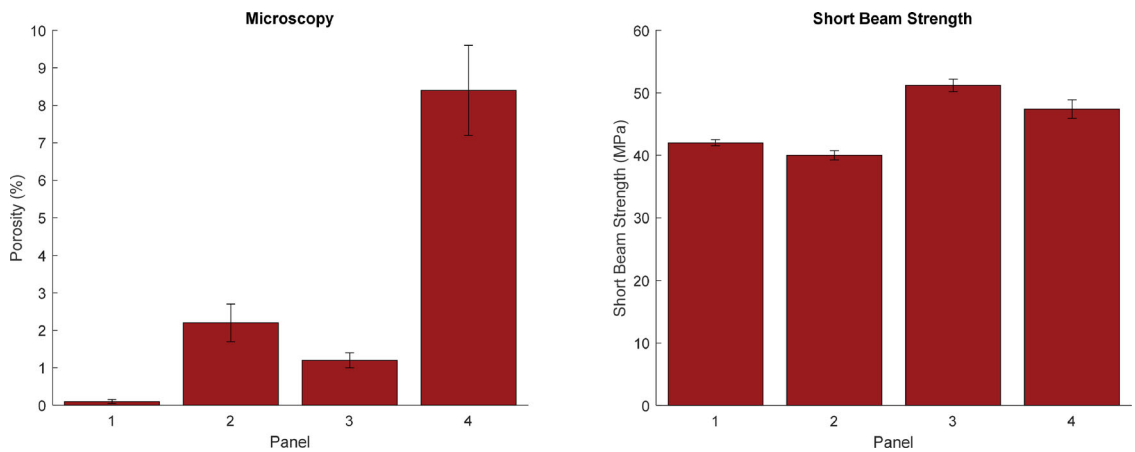

Figure 11. Quality and performance of fabricated panels. (a) Percent porosity. (b) Interlaminar shear strength.

Figure 11(b) highlights the differences between the ILSS of epoxy and vinyl hybrid. Panels 3 and 4 (epoxy panels), despite higher void contents than Panels 1 and 2 respectively, exhibited higher strength levels than the vinyl hybrid panels. The drop-off in strength between Panels 3 and 4 (due to porosity) was greater than the strength knockdown in Panels 1 and 2, a finding attributed to the higher levels of porosity [32]. The vinyl hybrid was a prototype resin, and strength levels inferior to epoxy laminates was not surprising.

4. Conclusions

Semi-preg formatting coupled with vinyl hybrid was demonstrated as an effective solution for robust patch repairs. The revised model for gel viscosity and subsequent flow number analysis was validated by comparing panels fabricated from semi-pregs featuring the vinyl hybrid resin to conventional prepregs with epoxy matrix. Normalized flow number analysis was used to design cure cycles that were used to perform a scarf repair on a custom tool plate that allowed *in situ* observations during cure. Video analysis from the repair tool confirmed the complementary effects of semi-preg format and vinyl hybrid resin on reducing porosity by simultaneously promoting gas evacuation and bubble migration. Panels exhibited porosity levels of 0–9% depending on the resin type and format used. The vinyl hybrid with semi-preg formatting exhibited the lowest void contents, while epoxy prepregs with conventional formatting showed the highest.

Cure profiles of resins that feature cure inhibition, low-viscosity, and fast-gelation/cure can be accurately predicted by modifying a conventional viscosity model, as demonstrated here. In this study, the conventional model predicted the viscosity profile of vinyl hybrid for much of the cure cycle, although the viscosity for the initial and final stages of cure was not accurately predicted. Accounting for this discrepancy is especially important for fast-cure resins such as vinyl hybrid, because such resins typically undergo short cure cycles that do not feature intermediate dwells. Consequently, such cure cycles effectively eliminate all but the initial and final stages of the typical viscosity profile. Accurate prediction of the initial and final stages of cure also is critical for calculation of flow number. Accurate modeling coupled with flow number analysis are required to design effective cure cycles that leverage the unusual properties of fast-cure resins for specific process requirements.

The material system presented in this work provides an opportunity to simplify and streamline repair processes and protocols, reducing minimal processing equipment. The use of resin that is stable at room-temperature obviates the requirement for freezer storage. Equally important, the semi-preg format eliminates the need for DVD processing, often required for wet layup and other repair procedures [15]. Although the vinyl hybrid matrix exhibits slightly lower strength than epoxy counterparts, the simplicity of processing, the consistency afforded by prepregs, and the relaxed storage requirements afford an opportunity to change how repairs can be performed, reducing maintenance logistics and depot footprints in so doing.

Acknowledgements

Vinyl hybrid film and consumables were donated by Tipton-Goss and Airtech International, respectively.

Disclosure statement

No potential conflict of interest was reported by the authors.

ORCID

David B. Bender http://orcid.org/0000-0001-6503-6221
Steven Nutt http://orcid.org/0000-0001-9877-1978

References

[1] Upadhya AR, Dayananda GN, Kamalakannan GM, et al. Autoclaves for aerospace applications: issues and challenges. Int J Aerosp Eng. 2011;2011:1–11.
[2] Hubert P, Fernlund G, Poursartip A. Autoclave processing for composites. In: Manufacturing techniques for polymer matrix composites (PMCs). Cambridge, UK: Elsevier; 2012. p. 414–434.
[3] Ridgard C, and S. for the A. of M. and P. Engineering, out of autoclave composite technology for aerospace, defense and space structures. Covina, CA: Society for the Advancement of Material and Process Engineering; 2009.
[4] Agius SL, Magniez KJC, Fox BL. Cure behaviour and void development within rapidly cured out-of-autoclave composites. Compos Part B Eng. 2013; 47:230–237.
[5] Cender TA, Gangloff JJJ, Simacek P, et al. Void reduction during out-of-autoclave thermoset prepreg composite processing. In: SAMPE Int. Symp.; 2013.
[6] Koushyar H, Alavi-Soltani S, Minaie B, et al. Effects of variation in autoclave pressure, temperature, and vacuum-application time on porosity and mechanical properties of a carbon fiber/epoxy composite. J Compos Mater. 2012;46(16): 1985–2004.
[7] Centea T, Hubert P. Out-of-autoclave prepreg consolidation under deficient pressure conditions. J Compos Mater. 2014;48(16):2033–2045.
[8] Arafath ARA, Fernlund G, Poursartip A. Gas transport in prepregs: model and permeability experiments. In: Proc. 17th Int. Conf. Compos. Mater., March 2015;

2009. p. 1–9. [Online]. Available from: http://www.iccm-central.org/Proceedings/ICCM17proceedings/Themes/Manufacturing/RESIDUALSTRESS&PROCE/C4.9Fernlund.pdf

[9] Kourkoutsaki T, Comas-Cardona S, Binetruy C, et al. The impact of air evacuation on the impregnation time of out-of-autoclave prepregs. Compos Part A Appl Sci Manuf. 2015;79:30–42.

[10] Archer E, McIlhagger A. Repair of damaged aerospace composite structures. In: Polymer composites in the aerospace industry. London: Elsevier; 2015. p. 393–412.

[11] Budhe S, Banea MD, de Barros S. Bonded repair of composite structures in aerospace application: a review on environmental issues. Appl Adhes Sci. 2018;6(1):1–27.

[12] Brassell GW, Horak JA, Butler BL. Effects of porosity on strength of carbon–carbon composites. J Compos Mater. 1975;9(3):288–296.

[13] Préau M, Hubert P. Processing of co-bonded scarf repairs: void reduction strategies and influence on strength recovery. Compos Part A Appl Sci Manuf. 2016;84:236–245.

[14] Wang PH. The comparison of composite aircraft field repair method (CAFRM) with traditional aircraft repair technologies. 2013.

[15] Barkoula NM, Alcock B, Cabrera NO, et al. Double-vacuum-bag technology for volatile management in composite fabrication. Polym Polym Compos. 2008;16(2):101–113.

[16] Chong HM, Liu SL, Subramanian AS, et al. Out-of-autoclave scarf repair of interlayer toughened carbon fibre composites using double vacuum debulking of patch. Compos Part A Appl Sci Manuf. 2018;107:224–234.

[17] NAVAIR. General composite repair. 2005.

[18] Gangloff JJ, Daniel C, Advani SG. A model of two-phase resin and void flow during composites processing. Int J Multiph Flow. 2014;65:51–60.

[19] Tungare AV, Martin GC, Gotro JT. Chemorheological characterization of thermoset cure. Polym Eng Sci. 1988;28(16):1071–1075.

[20] Mussatti FG, Macosko CW. Rheology of network forming systems. Polym Eng Sci. 1973;13(3):236–240.

[21] Macosko CW. Rheological changes during cross-linking. Br Poly J. 1985;17(2):239–245.

[22] Halley PJ, Mackay ME. Chemorheology of thermosets – an overview. Polym Eng Sci. 1996;36(5):593–609.

[23] Khoun L, Centea T, Hubert P. Characterization methodology of thermoset resins for the processing of composite materials – case study. J Compos Mater. 2010;44(11):1397–1415.

[24] Grunenfelder LK, Dills A, Centea T, et al. Effect of prepreg format on defect control in out-of-autoclave processing. Compos Part A Appl Sci Manuf. 2017;93:88–99.

[25] Schechter SGK, Grunenfelder LK, Nutt SR. Air evacuation and resin impregnation in semi-pregs: effects of feature dimensions. Adv Manuf Polym Compos Sci. 2020;6 (2):101–114.

[26] Schechter SGK, Centea T, Nutt SR. Polymer film dewetting for fabrication of out-of-autoclave prepreg with high through-thickness permeability. Compos Part A Appl Sci Manuf. 2018;114:86–96.

[27] Bendemra H, Compston P, Crothers PJ. Optimisation study of tapered scarf and stepped-lap joints in composite repair patches. Compos Struct. 2015;130:1–8.

[28] Gunnion AJ, Herszberg I. Parametric study of scarf joints in composite structures. Compos Struct. 2006;75(1–4):364–376.

[29] Bender DB, Centea T, Nutt S. Fast cure of stable semi-pregs via VBO cure. Adv Manuf Polym Compos Sci. 2020;6(4):245–255.

[30] Khoun L, Centea T, Hubert P. Characterization methodology of thermoset resins for the processing of composite materials — case study: CYCOM 890RTM epoxy resin. J Compos Mater. 2010;44(11):1397–1415.

[31] Min BG, Stachurski ZH, Hodgkin JH. Cure kinetics of elementary reactions of a diglycidyl ether of bisphenol A/diaminodiphenylsulfone epoxy resin: 2. Conversion versus time. Polymer (Guildf). 1993;34(21):4488–4495.

[32] Mehdikhani M, Gorbatikh L, Verpoest I, et al. Voids in fiber-reinforced polymer composites: a review on their formation, characteristics, and effects on mechanical performance. J Compos Mater. 2019;53(12):1579–1669.